Chemical and Process Engineering Research
ISSN 2224-7467 (Paper) ISSN 2225-0913 (Online)
Vol.44, 2016

Influence of Inclined Magnetic Field on Peristaltic Transport of Walters' B Fluid in an Inclined Asymmetric Channel with Porous Medium

Lika Z. Hummady * Ahmed M. abdulhadi
Department of Mathematics , college of science, University of Baghdad, Iraq

Abstract
This paper investigates the peristaltic motion of magneto hydrodynamic(MHD) non-Newtonian fluid in an inclined asymmetric channel with porous medium. Constitutive equations obeying the walter's B fluid model are employed. Mathematical modeling is developed in the presence of a constant inclined magnetic field making an angle with the vertical axis. Assumptions of long wave length approximation and low Reynolds number are used in flow analysis. Closed form expressions for the stream function and mechanical efficient are developed. Pressure rise per wave length and frictional force on the channel walls have been computed numerically. Effect of Hartman number, Froud number, Reynold number, permeability parameter , viscoelastic parameter and inclination of magnetic field on the axial velocity. Pumping and trapping are discussed in detail and shown graphically.
Keywords: Peristaltic Transport, Walter's B, Inclined Magnetic Field, Porous Medium, Inclined a symmetric channel, pimping ,trapping.

1 Introduction

Most of scientific problems and phenomena especially engineering and industry occur nonlinearly. Such as include extraction of crude oil from petroleum products, food mixing and chime movement in the intestine, flow of plasma, flow of blood, the movement of chime in the gastrointestinal tract, the vasomotion of small blood vessels, in roller and finger pumps and many others. After the seminal work of Latham(1966), several researchers have analyzed the phenomenon of peristaltic transport under various assumptions. It is noticed from the available literature that much has been reported on the peristaltic transport of hydrodynamic viscous and non-Newtonian fluids. Walter's B fluid model with limiting viscosity at low shear rates and short memory coefficient is beast model for the above mentioned situations. In industrial applications much attention(Beard and Walters 1964;Baris2002a,b;Nandeppanavar et al.2010;Joneidi et al.2010;Mohiddin etal.2010) have been paid to Walter,s B liquid but in physiological point of view only Nadeem and Akbar(2010) consider the peristaltic transport of Walter's B fluid in a uniform inclined tube. Keeping in mind the importance of symmetric/asymmetric nature of flow. Elshehawey et al.(2003)discussed the variation of inclined magnetic field effects on the flow of a viscous fluid saturating the porouse medium between two wavy porous plates. Flow through a porous medium has been of considerable interest in recent years, number of workers employing Darcy's law. (Rapit et al,1982, and Varshney,1979) have solved problems of the flow of a viscous fluid through a porous medium boundary by vertical surface. (Mekheimer and Al-Arabi, 2003), studied nonlinear peristaltic transport of MHD flow through a porous medium also (Mekheimer,2003) studied nonlinear peristaltic transport through a porous medium in an inclined planar channel. (Mekheimer and Abd Elmaboud,2008) investigated the peristaltic flow through a porous medium in an annulus. The purpose of the present work is to discuss the influence of an inclined magnetic field on peristaltic flow of Walter's B fluid. Here an incompressible fluid occupies the space in an inclined asymmetric channel. Series solutions of stream function, axial velocity are given by using regular perturbation technique when wave number is small. Numerical computations have been performed for the pressure rise, frictional forces and mechanical efficient . The variations of embedded flow parameters are discussed in detail.

2. Basic equation

The continuity and momentum equations in the absence of body forces for incompressible Walter's B fluid are

$$\text{div } V=0 \quad (1)$$

$$\rho \frac{dV}{d\bar{t}} = -\nabla\bar{p} + \text{div}\bar{S}, \quad (2)$$

Where V is the fluid velocity, $\frac{d}{d\bar{t}}$ is the material time derivative, ρ is the fluid density and $\bar{p}$ is the isotropic pressure. The extra stress tensor $\bar{S}$ for Walter's B fluid is defined by

$$\bar{S} = 2\eta_0 e - 2k_0 \frac{\delta e}{\delta t} \quad (3)$$

$$\frac{\delta e}{\delta t} = \frac{\delta e}{\delta t} + V.\nabla e - e\nabla V - (\nabla V)^T \boldsymbol{e} \quad (4)$$

Where e is the rat of strain tensor, $\frac{\delta e}{\delta t}$ is the convicted differentiation of the rate of strain tensor in relation to the material in motion and η_0 and k_0 are limiting viscosity at small shear rates and short memory coefficient respectively expressed by

$\eta_0 = \int_0^\infty N(\tau)d\tau,$ (5)

$k_0 = \int_0^\infty \tau N(\tau)d\tau,$ (6)

With $N(\tau)$ is the distribution function with relaxation time τ .By taking short memory into account the terms involving

$\int_0^\infty \tau N(\tau)d\tau, n \geq 2$, are neglected (Beard and Walters1964) in case of Walter'sB fluid.

3. problem description

Consider the tow dimensional flow of incompressible Walter 's B fluid in an asymmetric channel having width d_1+d_2. The flow is caused by infinite sinusoidal wave train moving ahead with constant velocity c along the walls of the channel. Different wave amplitudes, phase angle and channel widths result in an asymmetric channel.

The geometries of the walls are modeled as

$\bar{h}_1(\bar{X},\bar{t}) = d_1 + a_1 \sin[\frac{2\pi}{\lambda}((\bar{X} - c\,\bar{t})]$ upper wall, (7)

$\bar{h}_2(\bar{X},\bar{t}) = -d_2 - a_2 \sin[\frac{2\pi}{\lambda}((\bar{X} - c\,\bar{t}) + \Phi]$ lower wall, (8)

where a_1, a_2 , b, λ , c, Φ ,t, are the amplitudes of the waves , wavelength, wave speed, Φ ($0 \leq \Phi \leq \pi$) the phase difference and the rectangular coordinate system is chosen in such a way that $\bar{X}$-axis lies in the direction of wave propagation and $\bar{Y}$-axis perpendicular to $\bar{X}$ .It is noticed that Φ=0 corresponds to symmetric channel with waves out of phase and for $\Phi = \pi$ the waves are in phase. Further a_1, a_2,d_1,d_2 and Φ satisfy the condition.$a_1^2 + a_2^2 + 2a_1 a_2 \cos(\Phi) \leq (d1 + d2)^2$.

Fig.1.physical model

It is further assumed that there is no motion of walls in the longitudinal direction. This assumption restrict the deformation of the walls , it does not imply that the channel is rigid along the longitudinal motions.

The governing equation in the laboratory frame $(\bar{X},\bar{Y})$ can be written as

$$\frac{\partial \bar{U}}{\partial \bar{X}} + \frac{\partial \bar{V}}{\partial \bar{Y}} = 0 \quad (9)$$

$$\rho\left(\frac{\partial}{\partial \bar{t}} + \bar{U}\frac{\partial}{\partial \bar{X}} + \bar{V}\frac{\partial}{\partial \bar{Y}}\right)\bar{U} = -\frac{\partial \bar{P}}{\partial \bar{X}} + \frac{\partial}{\partial \bar{X}}\bar{S}_{\bar{X}\bar{X}} + \frac{\partial}{\partial \bar{Y}}\bar{S}_{\bar{X}\bar{Y}} - \sigma B_0^2 \cos\beta(\bar{U}\cos\beta - \bar{V}\sin\beta) + \rho g \sin\alpha - \eta_0 \frac{\bar{U}}{\overline{k1}} \quad (10)$$

$$\rho\left(\frac{\partial}{\partial \bar{t}} + \bar{U}\frac{\partial}{\partial \bar{X}} + \bar{V}\frac{\partial}{\partial \bar{Y}}\right)\bar{V} = -\frac{\partial \bar{P}}{\partial \bar{Y}} + \frac{\partial}{\partial \bar{X}}\bar{S}_{\bar{X}\bar{Y}} + \frac{\partial}{\partial \bar{Y}}\bar{S}_{\bar{Y}\bar{Y}} - \sigma B_0^2 \sin\beta(\bar{U}\cos\beta - \bar{V}\sin\beta) + \rho g \cos\alpha - \eta_0 \frac{\bar{V}}{\overline{k1}} \quad (11)$$

where

$S_{\bar{X}\bar{X}} = \eta_0(2\bar{U}_{\bar{X}}) - k_0(2\bar{U}_{\bar{X}\bar{t}} + 2\bar{U}\bar{U}_{\bar{X}\bar{X}} + 2\bar{V}\bar{U}_{\bar{X}\bar{Y}} - 4\bar{U}_{\bar{X}}^2 - 2\bar{V}_{\bar{X}}\bar{U}_{\bar{Y}} - 2\bar{V}_{\bar{X}}^2)$ (12)

$S_{\bar{X}\bar{Y}} = \eta_0(2\bar{U}_{\bar{Y}} + 2\bar{V}_{\bar{X}}) - k_0(\bar{U}_{\bar{Y}\bar{t}} + \bar{V}_{\bar{X}\bar{t}} + \bar{U}\bar{U}_{\bar{X}\bar{Y}} + \bar{U}\bar{V}_{\bar{X}\bar{X}} + \bar{V}\bar{U}_{\bar{Y}\bar{Y}} + \bar{V}\bar{V}_{\bar{Y}\bar{Y}} - 3\bar{U}_{\bar{X}}\bar{U}_{\bar{Y}} - \bar{V}_{\bar{Y}}\bar{U}_{\bar{Y}} - \bar{V}_{\bar{X}}\bar{U}_{\bar{X}} - 3\bar{V}_{\bar{X}}\bar{V}_{\bar{Y}})$ (13)

$S_{\bar{Y}\bar{Y}} = \eta_0(2\bar{V}_{\bar{Y}}) - k_0(2\bar{V}_{\bar{Y}\bar{t}} + 2\bar{U}\bar{V}_{\bar{X}\bar{Y}} + 2\bar{V}\bar{V}_{\bar{Y}\bar{Y}} - 2\bar{U}_{\bar{Y}}^2 - 2\bar{V}_{\bar{X}}\bar{U}_{\bar{Y}} - 4\bar{V}_{\bar{Y}}^2)$ (14)

where the ρ, ,$\bar{U},\bar{V}$, $\bar{Y}$, $\bar{p},\eta_0,k_0$ $\overline{k1}$, β_o , σ, g, are the fluid density ,axial velocity , transverse velocity, transverse coordinate , pressure, viscosity , material constant, permeability parameter, constant magnetic field, is the electrical conductivity, the acceleration due to gravity, and $S_{\bar{X}\bar{X}}$, $S_{\bar{X}\bar{Y}}$, $S_{\bar{Y}\bar{Y}}$, are the components of extra stress tensor. respectively. The flow is unsteady in the laboratory frame $(\bar{X},\bar{Y})$.

However in a coordinate system moving with the wave speed c(in wave frame$(\bar{x},\bar{y})$,the motion is steady. The following expressions

$\bar{x} = \bar{X} - c\bar{t}$, $\bar{Y} = \bar{y}$, $\bar{u} = \bar{U} - c$, $\bar{V} = \bar{v}$, $\bar{p}$ $((\bar{X},\bar{Y},\bar{t})$ (15)

where $\bar{u},\bar{v}$and $\bar{p}$ represent the velocity components and pressure in the wave frame.

To carry out the non-dimensional analysis we set up the following non-dimensional quantities

$x = \frac{\bar{x}}{\lambda}$,$y = \frac{\bar{y}}{d_1}$,$u = \frac{\bar{u}}{c}$, $v = \frac{\bar{v}}{c}$,,$h_1 = \frac{\bar{h}_1}{d_1}$,$h_2 = \frac{\bar{h}_2}{d_1}$ $P = \frac{\bar{p}{d_1}^2}{\eta_0 c\lambda}$,$k1 = \frac{\overline{k1}}{{d_1}^2}$, $Re = \frac{\rho c d_1}{\eta_0}$, $\delta = \frac{d_1}{\lambda}$, ,$M =$

$\sqrt{\frac{\sigma}{\eta_0}}\ d_1 B_o$, $S=\frac{d_1}{\eta_0 c}\bar{S}$, $K=\frac{k_0 c}{\eta_0 d_1}$

$$Fr = \frac{c^2}{d_1 g} \quad (16)$$

where δ ,is the wave number, Re the Renold number, K is the viscoelastic parameter, M the Hartman number, Fr is the Froude number

Then in view of Eqs(15)and(16), the Eqs(9)-(14) takes the form

$$\delta\frac{\partial u}{\partial x}+\frac{\partial v}{\partial y}=0 \quad (17)$$

$$Re\left(\delta u\frac{\partial u}{\partial x}+v\frac{\partial u}{\partial y}\right)=-\frac{\partial p}{\partial x}+\delta\frac{\partial S_{xx}}{\partial x}+\frac{\partial S_{xy}}{\partial y}-M^2\cos\beta(U\cos\beta-V\sin\beta)-\frac{Re}{Fr}\sin\alpha-\frac{u}{k1} \quad (18)$$

$$\delta Re\left(\delta u\frac{\partial v}{\partial x}+v\frac{\partial v}{\partial y}\right)=-\frac{\partial p}{\partial y}+\delta^2\frac{\partial S_{xy}}{\partial x}+\delta\frac{\partial S_{yy}}{\partial y}-\delta M^2\sin\beta(U\cos\beta-V\sin\beta)-\frac{Re}{Fr}\delta\cos\alpha-\frac{v}{k1} \quad (19)$$

$$S_{xx}=(2\delta u_x)-K(2\delta^2 uu_{xx}+2\delta vu_{xy}-4\delta u_x^2-2\delta v_x u_y-2\delta^2 v_x^2) \quad (20)$$

$$S_{xy}=(u_y+\delta v_x)-K(uu_{xy}+\delta^2 uv_{xx}+vu_{yy}+\delta vv_{xy}-3\delta u_x u_y-v_y u_y-\delta^2 v_x u_x-3\delta v_x v_y) \quad (21)$$

$$S_{yy}=(2v_y)-K(2\delta uv_{xy}+2vv_{yy}-2u_y^2-2\delta v_x u_y-4v_y^2) \quad (22)$$

The stream function ψ is found in the following relation with the velocity components

$$u=\frac{\partial\psi}{\partial y},\ v=-\delta\frac{\partial\psi}{\partial x}, \quad (23)$$

on using Eqs.(24), Eq.(17) is satisfied and Eqs.(18)-(19)becomes

$$Re\delta\left(\psi_y\frac{\partial}{\partial x}-\psi_x\frac{\partial}{\partial y}\right)\psi_y=-\frac{\partial p}{\partial x}+\delta\frac{\partial S_{xx}}{\partial x}+\frac{\partial S_{xy}}{\partial y}-M^2\cos\beta(\psi_y+1)\cos\beta+\delta\psi_x\sin\beta)-\frac{Re}{Fr}\sin\alpha-\frac{1}{k1}\psi_y \quad (24)$$

$$\delta^3 Re\left(\psi_y\frac{\partial}{\partial x}-\psi_x\frac{\partial}{\partial y}\right)\psi_x=-\frac{\partial p}{\partial y}+\delta^2\frac{\partial S_{xy}}{\partial x}+\delta\frac{\partial S_{yy}}{\partial y}+\delta M^2\sin\beta(\psi_y+1)\cos\beta+\delta\psi_x\sin\beta)-\frac{Re}{Fr}\delta\cos\alpha-\frac{\delta}{k1}\psi_x \quad (25)$$

Elimination of p between Eqs.(24)and (25) yields

$$Re\delta\left(\psi_y\frac{\partial}{\partial x}-\psi_x\frac{\partial}{\partial y}\right)\nabla^2\psi=\delta\left[\frac{\partial^2}{\partial x\,\partial y}(S_{xx}-S_{yy})\right]+\left[\frac{\partial^2}{\partial y^2}-\delta^2\frac{\partial^2}{\partial x^2}S_{xy}\right]-M^2\cos^2\beta\frac{\partial^2\psi}{\partial x\,\partial y}-\delta^2M^2\sin^2\beta\frac{\partial^2\psi}{\partial x^2}-\frac{1}{k1}(\psi_{yy}-\delta\psi_{xy}) \quad (26)$$

$$\nabla^2=\delta^2\frac{\partial^2}{\partial x^2}+\frac{\partial^2}{\partial y^2}$$

$$S_{xx}=(2\delta\psi_{xy})-K(2\delta^2\psi_y\psi_{xxy}-2\delta^2\psi_x\psi_{xyy}-4\delta\psi_{xy}^2+2\delta^2\psi_{xx}\psi_{yy}-2\delta^2\psi_{xx}^2) \quad (27)$$

$$S_{xy}=(\psi_{yy}-\delta^2\psi_{xx})-K(\delta\psi_y\psi_{xyy}-\delta^3\psi_y\psi_{xxx}-\delta\psi_x\psi_{yyy}+\delta^3\psi_x\psi_{xxy}-2\delta\psi_{xy}\psi_{yy}-2\delta^3\psi_{xx}\psi_{xy}) \quad (28)$$

$$S_{yy}=(-2\delta\psi_{xy})-K(2\delta^2\psi_y\psi_{xxy}+2\delta^2\psi_x\psi_{xyy}-2\psi_{yy}^2+2\delta^2\psi_{xx}\psi_{yy}-4\delta^2\psi_{xy}^2) \quad (29)$$

The dimensionless boundary conditions in the wave frame are (Haroun,2007b):

$$\psi=\frac{F}{2},\quad \frac{\partial\psi}{\partial y}=-1 \text{ at } y=h_1. \quad (30)$$

$$\psi=-\frac{F}{2},\quad \frac{\partial\psi}{\partial y}=-1 \text{ at } y=h_2. \quad (31)$$

Where F is the dimensionless time mean flow rate in the wave frame. It is related to the dimensionless time mean flow rate Q1 in the laboratory frame through the expression (Haroun,2007b)

$$Q1=F+1+d. \quad (32)$$

The dimensionless forms of $h_1(x)$ and $h_2(x)$ are

$$h_1(x)=1+a\sin x,\qquad h_2(x)=-d-b\sin(x+\Phi), \quad (33)$$

where a ,b, Φ and d satisfy (Haroun,2007b):

$$a^2+b^2+2ab\cos\Phi\ \le(1+d)^2. \quad (34)$$

4.Solution of the problem

Eq.(26) is highly non-linear and complicated; therefore it is impossible to obtain closed form solution for all the involving arbitrary parameters . Even for Newtonian fluid the solution is obtained under certain assumptions and approximations. In tubs or channels of small diameters the wave length as compared to the tube diameter($d_1 \le \lambda$) giving small wave number $\delta \le 1$. The assumption of small wave number is appropriate in study of peristaltic flows in tubes or channel of small diameter (Shapiro et al.1969) and is used by many researchers (Hayat et al. 2008; Nadeem and Akbar 2010;Ravikumar et al. 2010b; Mehmood et al.2011) with this fact in view, to seek the convergent solution for small wave number δ we expand the flow quantities in term of small wavenumberδ ($\delta \le 1$).

$$\psi = \psi_0 + \delta\psi_1 + O(\delta^2)$$
$$F = F_0 + \delta F_1 + O(\delta^2)$$
$$p = p_0 + \delta p_1 + O(\delta^2)$$
$$S = S_0 + \delta S_1 + O(\delta^2) \quad (35)$$

And substitute the expressions (35) into Eqs. (24)-(29) with boundary conditions (30)-(31) since $\delta \leq 1$, the higher order terms involving the powers of δ are smaller and thus negligible giving convergent solution. On comparing the coefficients of powers of δ we obtain as follows

4.1 Zero order system

The zeroth order system is

$$\frac{\partial^2 S_{0xy}}{\partial y^2} - m^2\psi_{0yy} = 0 \quad (36)$$
$$m^2 = M^2\cos^2\beta - \frac{1}{k1} \quad (37)$$
$$\frac{\partial p_0}{\partial x} = \frac{\partial}{\partial y}S_{0xy} - m^2(\psi_y + 1) + \frac{Re}{Fr}\sin\alpha, \quad (38)$$
$$\frac{\partial p_0}{\partial y} = 0 \quad (39)$$
$$S_{0xy} = \psi_{0yy},\ S_{0xx} = 0,\ S_{0yy} = 2K\psi_{0yy}^2 \quad (40)$$
$$\psi_0 = \frac{F_0}{2}, \quad \frac{\partial\psi_0}{\partial y} = -1 \text{ at } y = h_1. \quad (41)$$
$$\psi_0 = -\frac{F_0}{2}, \quad \frac{\partial\psi_0}{\partial y} = -1 \text{ at } y = h_2. \quad (42)$$

4.2 First order system

$$Re\delta\left(\psi_{0y}\Psi_{0yyx} - \Psi_{0x}\Psi_{0yyy}\right) = -\left[\frac{\partial^2}{\partial x\,\partial y}\left(S_{0yy}\right)\right] + \left[\frac{\partial^2}{\partial Y^2}S_{1xy}\right] - M^2\,Cos^2\beta\,\psi_{1yy} - M^2\,Cos\,\beta\,sin\beta\psi_{0xy} - \frac{1}{k1}(\Psi_{0xy} - \Psi_{1yy})) \quad (43)$$
$$\frac{\partial p_1}{\partial x} = \frac{\partial}{\partial y}S_{1xy} - m^2(\psi_{1y} + 1) + \psi_{0x}\sin\beta - Re(\psi_{0y}\Psi_{0yx} - \Psi_{0x}\Psi_{0yy}), \quad (44)$$
$$S_{1xy} = (\psi_{1yy}) - K(\psi_{0y}\psi_{0xyy} - \psi_{0x}\psi_{0yyy} - 2\psi_{0xy}\psi_{0yy}) \quad (45)$$
$$S_{xx} = (2\psi_{0xy}) + K(4\psi_{0xy}^2) \quad (46)$$
$$S_{yy} = (-2\psi_{0xy}) + K(2\psi_{1yy}^2) \quad (47)$$
$$\psi_1 = \frac{F_1}{2}, \quad \frac{\partial\psi_1}{\partial y} = -1 \text{ at } y = h_1. \quad (48)$$
$$\psi_1 = -\frac{F_1}{2}, \quad \frac{\partial\psi_1}{\partial y} = -1 \text{ at } y = h_2. \quad (49)$$

Then solving the corresponding zeroth and first order system we obtain the final expressions for the stream function,

$$\psi = (A1 + A2y + A3\frac{e^{my}}{m^2} + A4\frac{e^{-my}}{m^2}) + \delta(\frac{1}{24k1m^4}e^{-2my}(6C3e^{3my}(-5 + 2my) - 6C4e^{my}(5 + 2my) + m(A4k1m(3B2e^{my}(-Re(17 + 10my + 2m^2y^2) + Km(17 + 10m(4 + y) + 2m^2y(8 + y))) + 2m(B4K(-1 + m)m + 3e^{my}(2B3e^{my}Km^3(1 + 3m)y^2 + B1(Km - Re)(5 + 2my)))) - e^{my}(A3e^{my}k1m(2m(3B1e^{my}(Km + Re)(-5 + 2my) + Km(B3e^{2my}(1 + m) + 6B4m^2(-1 + 3m)y^2)) + 3B2e^{my}(RE(17 - 10my + 2m^2y^2) + Km(17 - 10m(4 + y) + 2m^2y(8 + y)))) + 2(-15B3e^{2my}k1r + 6B3e^{2my}k1mry + 6C1e^{my}my^2 - 6B2e^{my}k1mry^2 + 2C2e^{my}my^3 + 3B4k1r(5 + 2my) + 3A2k1m(Km^2 + Re)(-B3e^{2my}(-5 + 2my) + B4(5 + 2my)) - 12e^{2my}k1mA11 - 12k1mA12)))) + A13 + yA14) \quad (50)$$

The function (A1,A2,A3,A4,A11,A12,A13,A14,B1,B2,B3,B4,C1,C2,C3,C4,r) are large expressions will not mentioned here for sake of simplify.

$$\frac{\partial p}{\partial x} = (\frac{\partial}{\partial y}S_{0xy} - m^2(\psi_{0y} + 1) + \frac{Re}{Fr}\sin\alpha) + (\frac{\partial}{\partial y}S_{1xy} - m^2(\psi_{1y} + 1) + \psi_{0x}\sin\beta - Re(\psi_{0y}\psi_{0xy} - \psi_{0x}\psi_{0yy}) \quad (51)$$

The axial velocity component in the fixed frame is given as

$$U(X,Y) = 1 + \psi_y \quad (52)$$

The pressure rise per wave length (Δp) and frictional force on the lower(F^1) and upper(F^{11}) walls are defined as

$$\Delta p = \int_0^1 \frac{\partial p}{\partial x}\,dx, \quad (53)$$
$$F^1 = \int_0^1 h_2^2\,(-\frac{\partial p}{\partial x})dx. \quad (54)$$
$$F^{11} = \int_0^1 h_1^2\,(-\frac{\partial p}{\partial x})dx. \quad (55)$$

The mechanical efficiency is the ratio of the average rate per wavelength at which work is done by the moving fluid against a pressure head and the average rate at which the walls do work on the fluid. It is derived as

$$E = -\frac{\overline{Q}\,\Delta P}{\phi I}, \quad (56)$$

Where

$$I=\int_0^1 \frac{\partial P}{\partial x}\sin(2\pi x)\,dx. \quad (57)$$

3. Result and discussion

We have divided this section into three subsections. In the first subsection the effects various parameters of interest on the pumping characteristics are investigated. The flow characteristics are discussed in the second subsection. In the last subsection trapping phenomenon is illustrated using the software Mathematic. These results are good agreement with those reported by (Hayat et.al.2010; Mehmood et al 2011)

3.1 pumping characteristic

This sub section describes the effects of Hart man number (M), Froud number(Fr),inclination of the channel (α),viscoelastic parameter(K), Renolds number (Re), phase difference (Φ), permeability parameter (k1),occlusion parameter (a). The dimensionless axial pressure rise per wave length (Δp) is plotted against the dimensionless average flux Q1 for different values of parameters. We divided the whole region into four parts as follows:

1) Peristaltic pumping region where $(\Delta p) > 0$ and $Q1 > 0$.
2) There is augmented pumping region when $(\Delta p) < 0$ and $Q1 > 0$.
3) When $(\Delta p) > 0$and$Q1 < 0$ then there is retrograde pumping region.
4) $(\Delta p) = 0$ corresponds to the free pumping region.

Fig.2shows that all pumping regions decrease by increasing(Fr). Fig.3 shows the effect of sin α on(Δp). It is notice that (Δp) increases with sin α or angle of inclination of the channel. This mean that in this case all the pumping regions increase when $(\sin\alpha)$ increase. Fig.3indicates that the pumping rate increasing by increasing (M). However after critical value of Q1 that is Q1=-8.89, the pumping rate decreases when(M)increased. Fig.4 shows that all pumping regions increase when(Re) increase. Fig.5 No significant variation is found in pumping with the change in(K) and so Fig.8. No significant variation is found in pumping with the change in (β). In Fig.7indicates that the pumping rate increases by increasing (k1). However after critical value of Q1 that Q1=-25, the pumping rate decreases when k1 increased. Fig. 9 Δp decreases with increases (Φ) at Q1< 5 and for Q1>5, (Δp) has an opposite behavior as well as Fig.11 Δp decreases with increases (b) at Q1<-1.5 and increases when Q1>-1.5. In Fig.10 the pumping rate increases with increases (a) for Q1<10 and decreases for Q1>10.

3.2 Frictional forces

The behavior of frictional force is observed under the influence of K, Re, M, k1, sinα, Fr, β, Φ, a and b at both upper and lower walls, Numerical integration is performed over the domain [0.1] and graphs are plotted.

Frictional force F^{11} and F^{1} are plotted in Figs(12-21) against the dimensionless average flux Q1 different values of parameters at upper and lower walls of the channel respectively. Fig.12. It is observed that frictional force decreases at upper wall and increases at lower wall with increases in (K). Fig.13. Highlights the variation of F^{11} and F^{1} against the dimensionless average flux Q1 for different values of (Re) at the upper and lower walls of the channel. It is seen that frictional force increases at upper wall and decreases at lower wall for increasing (Re). Figs(14-15) show that increases the frictional force at Q1<5 and decreases for Q1>5 at the upper wall and the lower wall respectively with increasing (M)or(k1). In Fig.16. we can show that decreases the frictional force at the upper wall and the lower wall with increasing(sinα), but in Fig.17 the frictional force have an opposite behavior with increasing (Fr). In Fig.18. we noticed that the effect of (β) parameter very small on frictional force both upper and lower wall. Fig.19. show that increases the frictional force at upper wall and lower wall respectively with increasing (Φ). Fig.20. the frictional force have an opposite behavior with increasing (a) and in Fig.21. show that the frictional force decreases forQ1<10 and increases for Q1>10 for both upper and lower wall with increasing (b).

3.3 mechanical efficient

Using Eqs, (53),(56) and (57), we draw graphs(Figs.22-31) between mechanical efficiency (E) and the average flow rate Q1 to study the variations of mechanical efficiency for different physical parameters (K, Re, M, k1, sinα, Fr, β, Φ, a and b). In Fig22. We can show that no effect mechanical efficiency with different values of (K). Fig.23. It noticed that mechanical efficiency decreases for Q1<6 and increases for Q1>6 with increasing (Re). In Fig.24. shows that mechanical efficiency decreases with increasing (M), but in Fig.26. mechanical efficiency has an opposite behavior with increasing (sinα). Figs.(25),(27) show that increasing mechanical efficiency for

Q1<0.98 and decreasing for Q1>0.98 with increasing (k1)and (Fr). In Fig.28. we noticed that decreases in mechanical efficiency with increasing (β). Fig.29.showe that decreases mechanical efficiency for Q1<4 and increases for Q1>4 with increasing (Φ). Fig30. Mechanical efficiency increasing for Q1<7.8 and decreasing for Q1>7.8 with increasing (a) and in Fig.31 we can show that increasing in mechanical efficiency with increasing (b).

3.4 Flow characteristics

The aim of this subsection is to explain the effects of M and inclination β of the magnetic field on the axial velocity profile and effects for each K , Re , k1,Q1,Φ,a,b,d. It should be noted that an inclination of the channel does not affect the velocity field. It effect only the pressure field. Fig.32. show that reduce the velocity with increasing (K). In Fig. 33. show that not effect the axial velocity with different values of (Re). Fig.34.show that the increasing in velocity for y<6and reduce for y>6 with increasing M . In Fig35. We can show that the axial velocity increases for y<4 and reduce for y>4 with increasing (k1). Fig .36. notice that the axial velocity increases with increasing(Q1). Fig.37.show that the axial velocity decreases for y<4 and increases for y>4 with increasing (Φ). In Fig. 38.shoe that not effect the velocity with different value of (β). Fig 39. Show that the velocity decreases for y<4 and increases for y>4 with increasing (a). In Fig.40. notice that the velocity increases for y<0 and decreases for y>0 with increasing (b) and in Fig.41. show that the velocity increases for y<-6 and decreases for y>-6 with increasing (d). And we can show that for the plots of axial velocity , the maximal velocity in the middle channel.

3.5 Trapping

An interesting phenomenon occurs in the peristaltic flows i.e. the closed stream lines trap the amount of fluid usually called bolus inside the channel /tube near walls and this trapping bolus moves ahead in the direction of the wave propagation. The stream lines are plotted for different values of K , Re , k1 ,M, $\beta, Q1,$ in the symmetric(upper panel Φ=0) and asymmetric(lower panel Φ =$\frac{\pi}{3}$) channels. In Figs.42-43. The stream lines are plotted for different vale of K and Re respectively. These figures exhibits that the trapping exist for both upper and lower walls and the trapping is symmetric along the center line of the channel. In this Figs. It is seen that with increase in K , Re the trapping reduces and this reduction is sharp near the walls. For large K , Re trapping vanishes. To examine the effects of Hartman number (M) , permeability parameter(k1) , the inclination of magnetic field(β)and average flow rate(Q1)in Figs.44-47.we can show that for all the plots the stream lines near the channel do nearly strictly follow the wall waves , which are mainly engendered by the relative movement of the walls. We observe that the size of the tapping bolus decreases for both the symmetric and the asymmetric cases when this parameters (M,k1,β,Q1)increased.

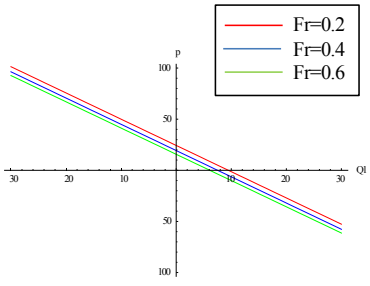

Fig.2. variation of Q1 withΔp for different value of Fr at M=1 , K=0.1,β=0.1,Re=10, K1=0.2, Sinα=0.5,Φ=0.55,a=0.5,b=0.5,d=1

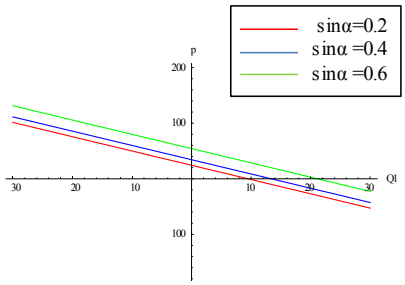

Fig.3. variation of Q1 withΔp for different value of Sinα at M=1 , K=0.1,β=0.1,Re=10, K1=0.2, Fr=0.5,Φ=0.55,a=0.5,b=0.5,d=1

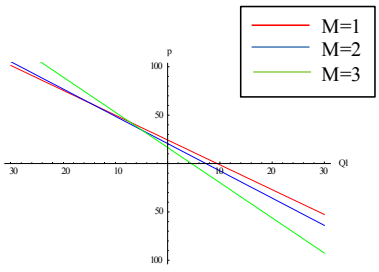

Fig4.. variation of Q1 withΔp for different value of M at Fr =0.2 , K=0.1,β=0.1,Re=10, K1=0.2, Sinα=0.5,Φ=0.55,a=0.5, b=0.5,d=1

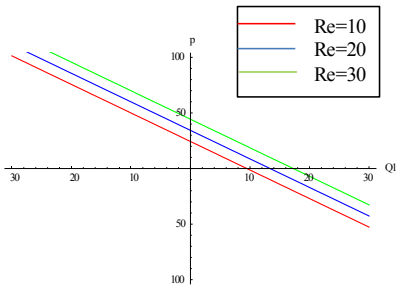

Fig.5. variation of Q1 withΔp for different value of Re at M=1 , K=0.1,β=0.1,Fr=0.2, K1=0.2, Sinα=0.5,Φ=0.55,a=0.5,b=0.5,d=1

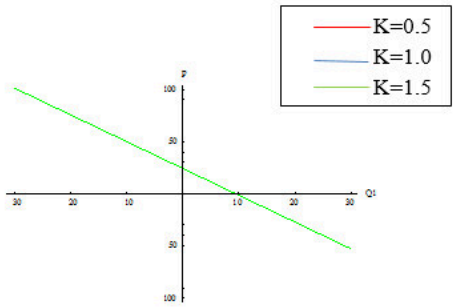

Fig.6. variation of Q1 withΔp for different value of K at M=1 , Fr=0.2,β=0.1,Re=10, K1=0.2, Sinα=0.5,Φ=0.55,a=0.5,b=0.5,d=1

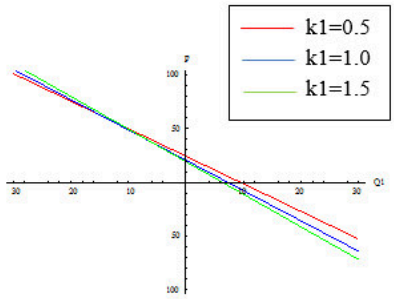

Fig.7. variation of Q1 withΔp for different value of K1 at M=1 , K=0.1,β=0.1,Re=10, Fr=0.2, Sinα=0.5,Φ=0.55,a=0.5,b=0.5,d=1

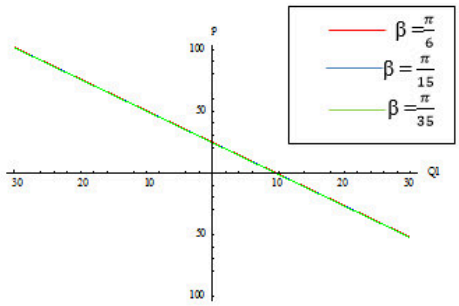

Fig.8. variation of Q1 withΔp for different value of β at M=1 , K=0.1, Fr=0.2,Re=10, K1=0.2, Sinα=0.5,Φ=0.55,a=0.5,b=0.5,d=1

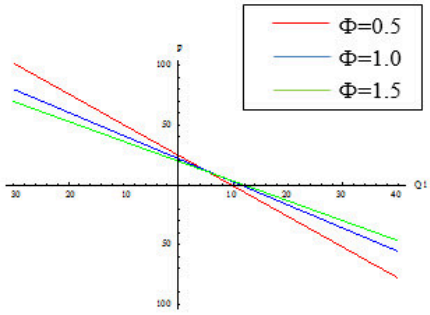

Fig.9. variation of Q1 withΔp for different value of Φ at M=1 , K=0.1,β=0.1,Re=10, K1=0.2, Sinα=0.5,Fr =0.2,a=0.5,b=0.5,d=1

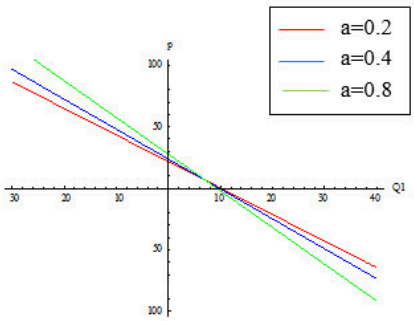

Fig.10. variation of Q1 withΔp for different value of a at M=1 , K=0.1,β=0.1,Re=10, K1=0.2, Sinα=0.5,Φ=0.55,Fr=0.2,b=0.5,d=1

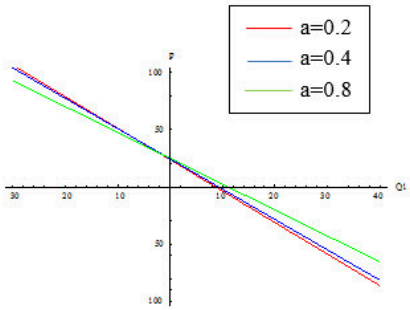

Fig.11. variation of Q1 withΔp for different value of b at M=1 , K=0.1,β=0.1,Re=10, K1=0.2, Sinα=0.5,Φ=0.55,a=0.5,Fr=0.2,d=1

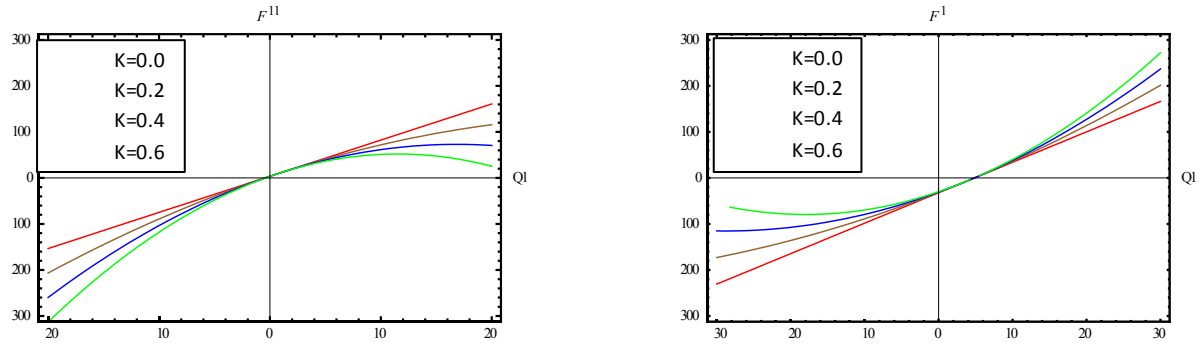

Fig.12. Effect of **K** on variation Q1with (F^{11}) at upper wall and (F^{1}) at lower wall when Re=5 ,M=1, k1=0.2, Sinα=0.2, Fr = 0.2,β =$\frac{\pi}{6}$,Φ =0.5, a =0.5,b =0.5 ,d=1

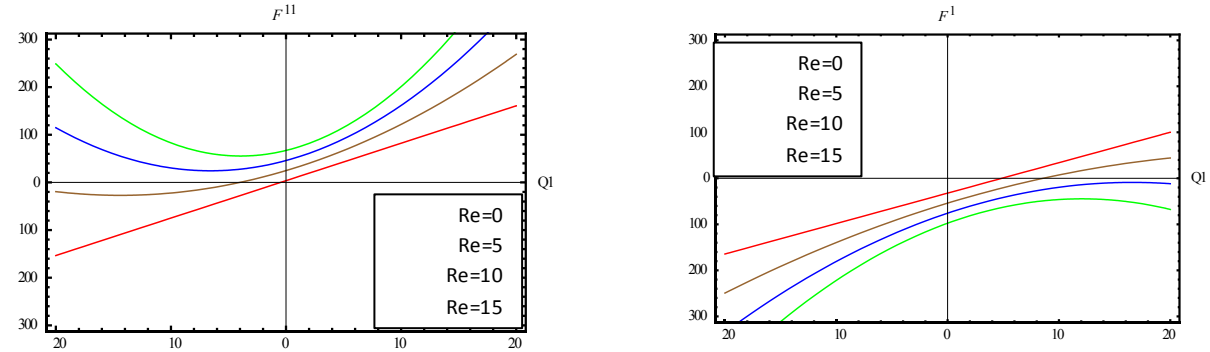

Fig.13. Effect of **Re** on variation Q1with (F^{11}) at upper wall and (F^{1}) at lower wall when K= 0.2 ,M=1, k1=0.2, Sinα=0.2, Fr = 0.2,β =$\frac{\pi}{6}$,Φ =0.5, a =0.5,b =0.5 ,d=1

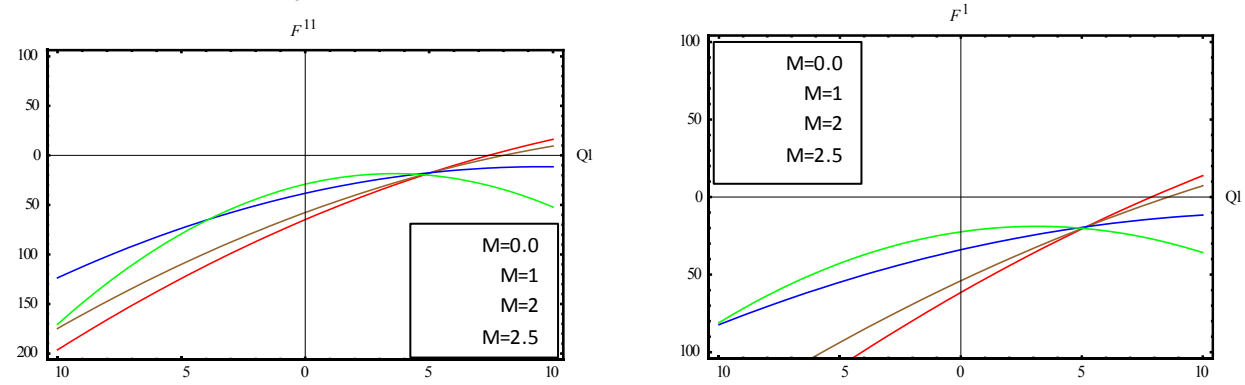

Fig.14. Effect of **M** on variation Q1with (F^{11}) at upper wall and (F^{1}) at lower wall when Re=5 ,K=0.2, k1=0.2, Sinα=0.2, Fr = 0.2,β =$\frac{\pi}{6}$,Φ =0.5, a =0.5,b =0.5 ,d=1

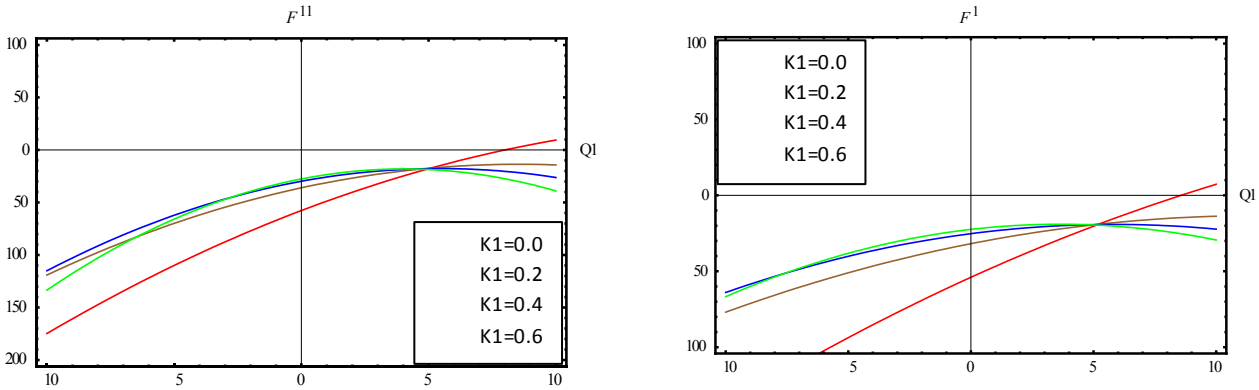

Fig.15. Effect of **k1** on variation Q1with (F^{11}) at upper wall and (F^{1}) at lower wall when Re=5 ,M=1,K=0.2, Sinα=0.2, Fr = 0.2,β =$\frac{\pi}{6}$,Φ =0.5, a =0.5,b =0.5 ,d=1

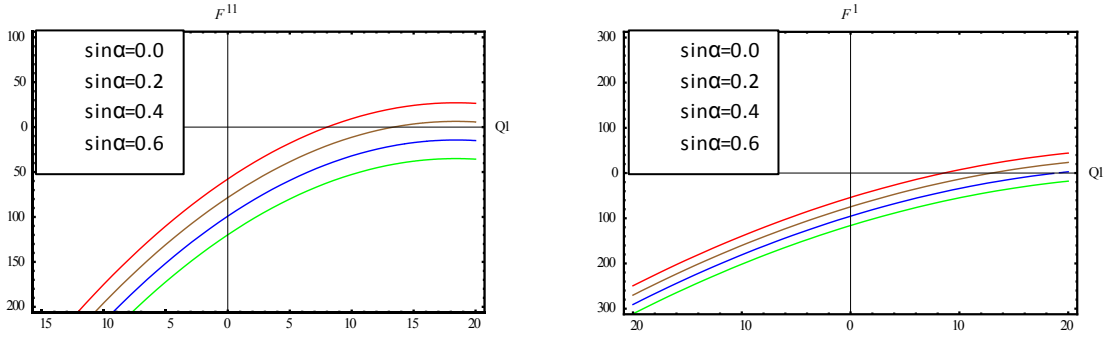

Fig.16. Effect of **Sinα** on variation Q1with (F^{11}) at upper wall and (F^{1}) at lower wall when Re=5 ,M=1, k1=0.2, K =0.2, Fr = 0.2,β =$\frac{\pi}{6}$,Φ =0.5, a =0.5,b =0.5 ,d=1

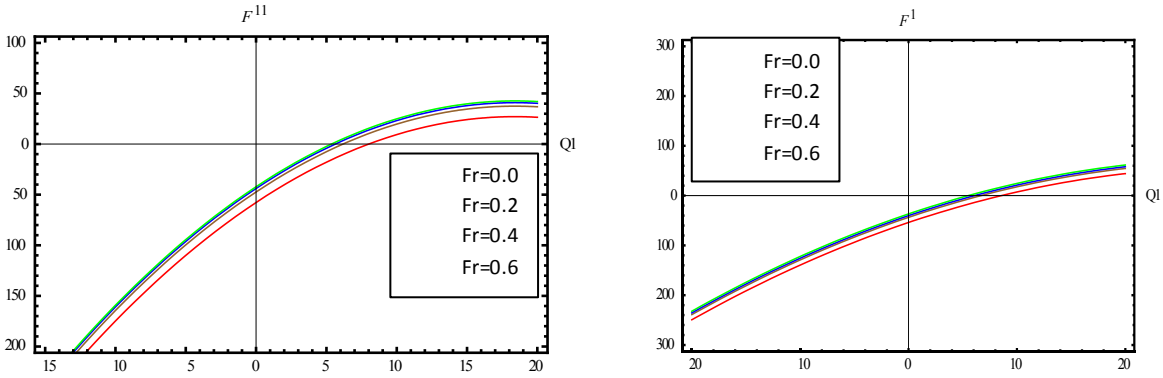

Fig.17. Effect of **Fr** on variation Q1with (F^{11}) at upper wall and (F^{1}) at lower wall when Re=5 ,M=1, k1=0.2, Sinα=0.2,K = 0.2,β =$\frac{\pi}{6}$,Φ =0.5, a =0.5,b =0.5 ,d=1

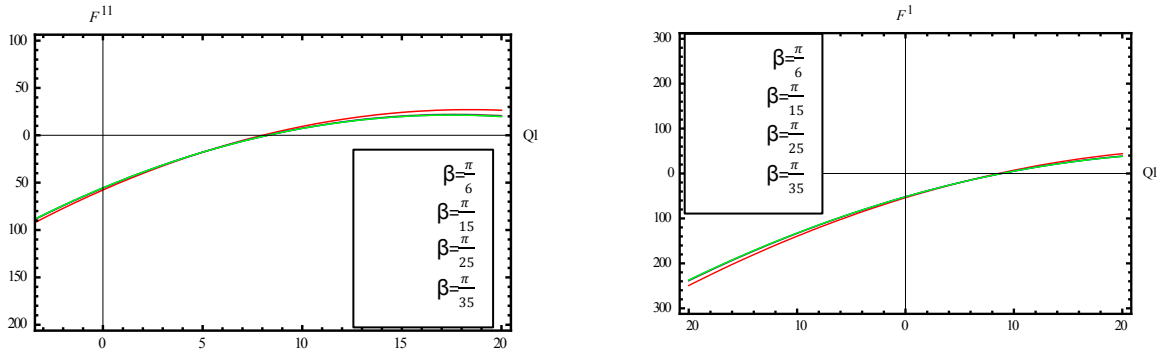

Fig.18. Effect of **β** on variation Q1with (F^{11}) at upper wall and (F^{1}) at lower wall when Re=5 ,M=1, k1=0.2, Sinα=0.2, Fr = 0.2, K =0.2 ,Φ =0.5, a =0.5,b =0.5 ,d=1

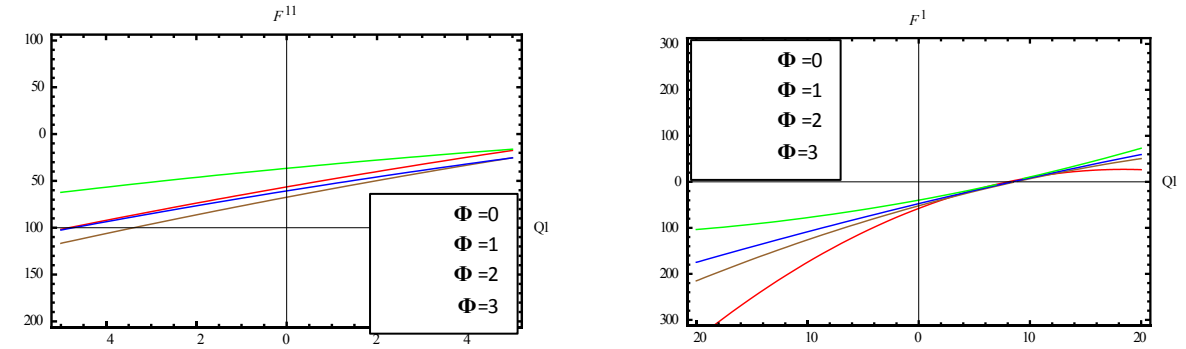

Fig.19. Effect of **Φ** on variation Q1 with (F^{11}) at upper wall and (F^{1}) at lower wall when Re=5 ,M=1, k1=0.2, Sinα=0.2, Fr = 0.2,β =$\frac{\pi}{6}$,K =0.2, a =0.5, b =0.5 , d=1

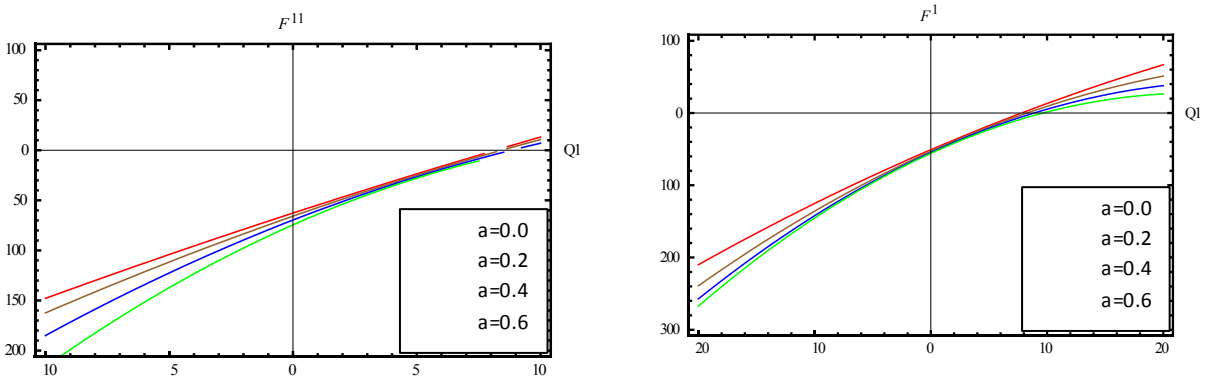

Fig.20. Effect of **a** on variation Q1with (F^{11}) at upper wall and (F^{1}) at lower wall when Re=5 ,M=1, k1=0.2, Sinα=0.2, Fr = 0.2,β =$\frac{\pi}{6}$,Φ =0.5, K =0.2,b =0.5 ,d=1

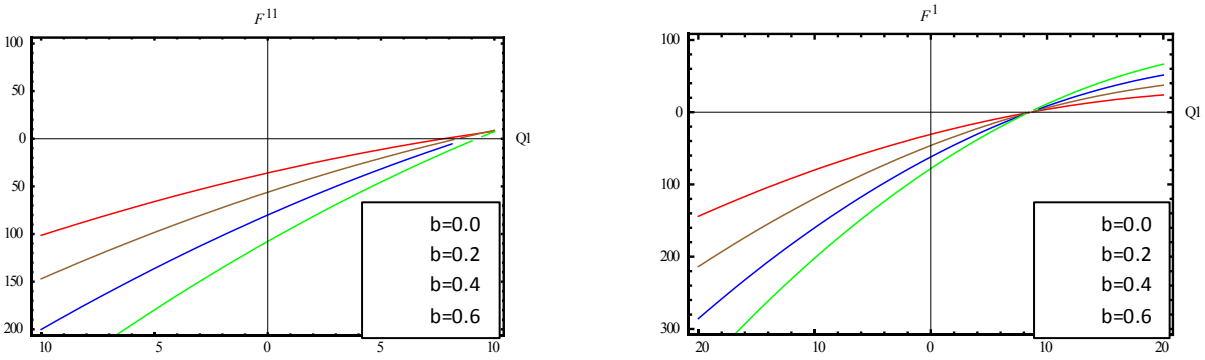

Fig.21. Effect of **b** on variation Q1with (F^{11}) at upper wall and (F^{1}) at lower wall when Re=5 ,M=1, k1=0.2, Sinα=0.2, Fr = 0.2,β =$\frac{\pi}{6}$,Φ =0.5, a =0.5,K =0.2 ,d=1

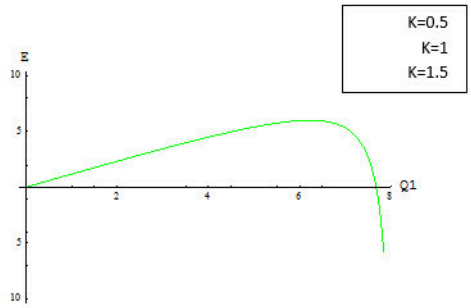

Fig. 22. Mechanical Efficiency versus averaged flow rate for various value of **K** at Re=5, M=1, k1=0.2,Sinα=0.2,Fr=0.2, β =$\frac{\pi}{6}$,Φ=0.5 , a=0.5,b=0.5,d=1.

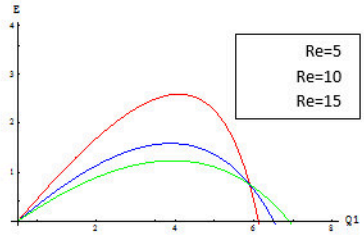

Fig. 23. Mechanical Efficiency versus averaged flow rate for various value of **Re** at K=0.2, M=1, k1=0.2,Sinα=0.2,Fr=0.2, β =$\frac{\pi}{6}$,Φ=0.5 , a=0.5,b=0.5,d=1.

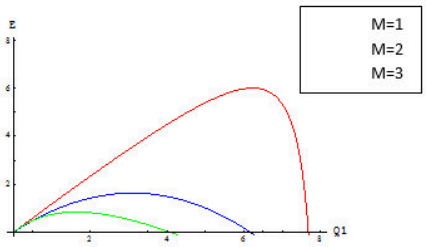

Fig. 24. Mechanical Efficiency versus averaged flow rate for various value of **M** at Re=5,K=0.2, k1=0.2,Sinα=0.2,Fr=0.2, β =$\frac{\pi}{6}$,Φ=0.5 , a=0.5,b=0.5,d=1.

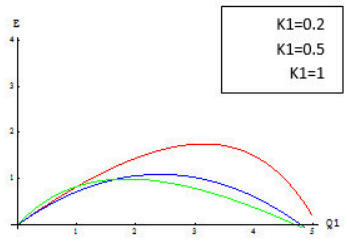

Fig. 25. Mechanical Efficiency versus averaged flow rate for various value of **k1** at Re=5, M=1, K=0.2,Sinα=0.2,Fr=0.2, β =$\frac{\pi}{6}$,Φ=0.5 , a=0.5,b=0.5,d=1.

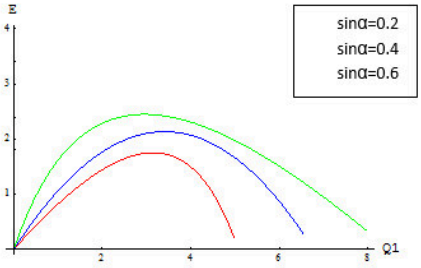

Fig. 26. Mechanical Efficiency versus averaged flow rate for various value of **Sinα** at Re=5, M=1, k1=0.2, K =0.2,Fr=0.2, β =$\frac{\pi}{6}$,Φ=0.5 , a=0.5,b=0.5,d=1.

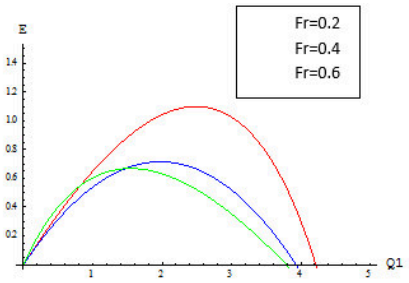

Fig. 27 Mechanical Efficiency versus averaged flow rate for various value of **Fr** at Re=5, M=1, k1=0.2,Sinα=0.2,K=0.2, β =$\frac{\pi}{6}$,Φ=0.5 , a=0.5,b=0.5,d=1.

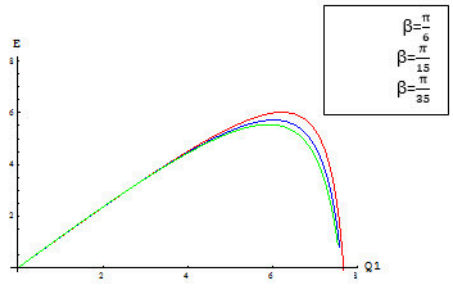

Fig. 28 Mechanical Efficiency versus averaged flow rate for various value of **β** at Re=5, M=1, k1=0.2,Sinα=0.2,Fr=0.2,K =0.2,Φ=0.5 , a=0.5,b=0.5,d=1.

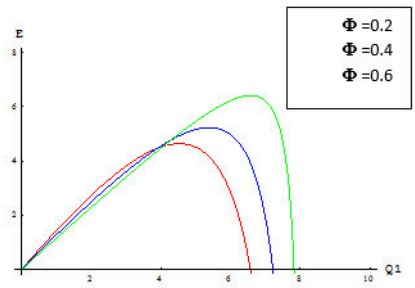

Fig. 29 Mechanical Efficiency versus averaged flow rate for various value of **Φ** at Re=5, M=1, k1=0.2,Sinα=0.2,Fr=0.2,K =0.2,β =$\frac{\pi}{6}$, a=0.5,b=0.5,d=1.

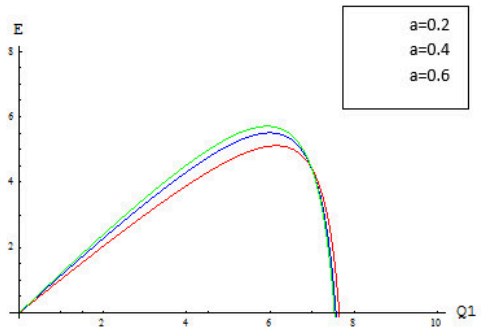

Fig. 30. Mechanical Efficiency versus averaged flow rate for various value of **a** at Re=5, M=1, k1=0.2,Sinα=0.2,Fr=0.2,K =0.2,β =$\frac{\pi}{6}$, Φ=0.5,b=0.5,d=1.

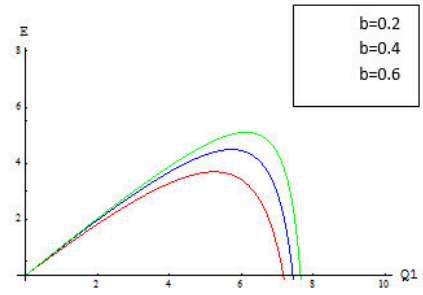

Fig. 31. Mechanical Efficiency versus averaged flow rate for various value of **b** at Re=5, M=1, k1=0.2,Sinα=0.2,Fr=0.2,K =0.2,β =$\frac{\pi}{6}$, a=0.5,Φ=0.5,d=1.

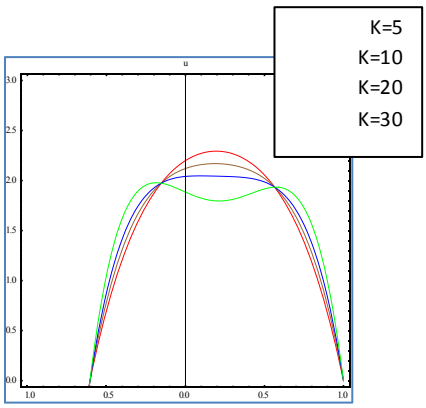

Fig.32.the velocity for different values of **K** at M=1.5,Re=5,Q1=1.1, k1=0.2,Φ=0.5, a=0.2, b=0.2,d=0.5

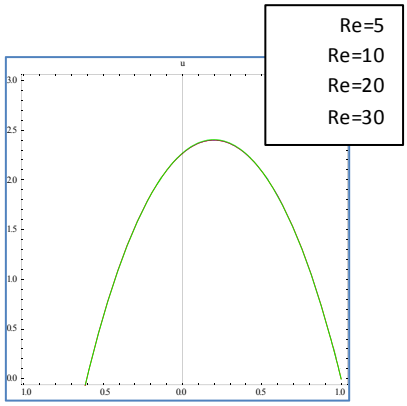

Fig.33.the velocity for different values of **Re** at M=1.5,K=0.2 ,Q1=1.1,k1=0.2,Φ=0.5, a=0.2, b=0.2.d=0.5

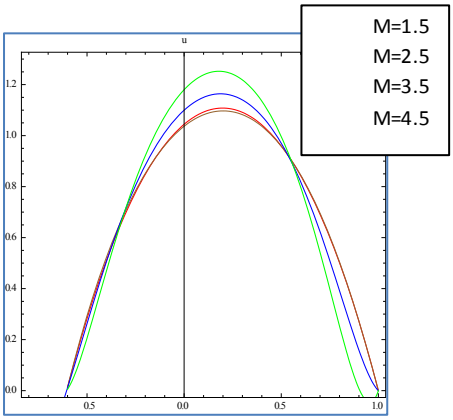

Fig.34.the velocity for different values of **M** at K=1.2 ,Re=5,Q1=1.1,k1=0.2,Φ=0.5, a=0.2, b=0.2.d=0.5

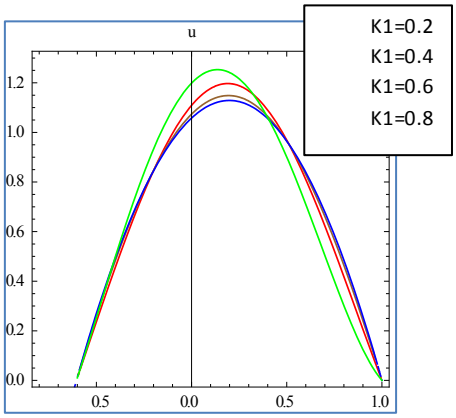

Fig.35.the velocity for different values of **k1** at M=1.5,Re=5,Q1=1.1,k1=0.2,Φ=0.5, a=0.2, b=0.2.d=0.5

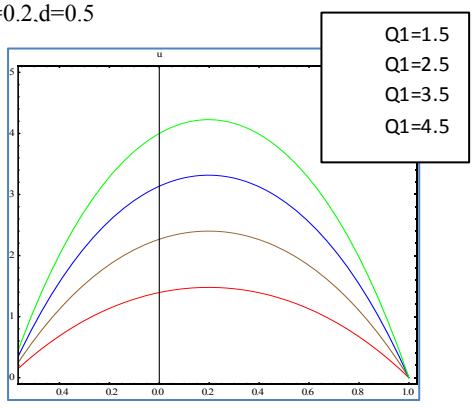

Fig.36.the velocity for different values of **Q1** at M=1.5,Re=5,Q1=1.1,k1=0.2,Φ=0.5, a=0.2, b=0.2.d=0.5

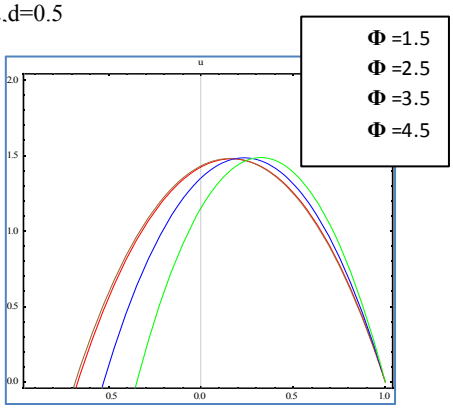

Fig.37.the velocity for different values of **Φ** at M=1.5,Re=5,Q1=1.1,,k1=0.2,Φ=0.5, a=0.2, b=0.2.d=0.5

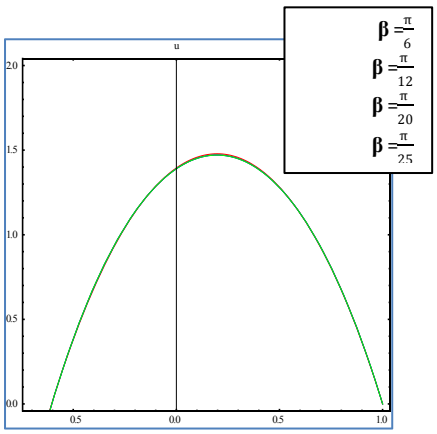

Fig.38.the velocity for different values of **β** at M=1.5,Re=5,Q1=1.1,Φ=0.5, a=0.2, b=0.2,d=0.5

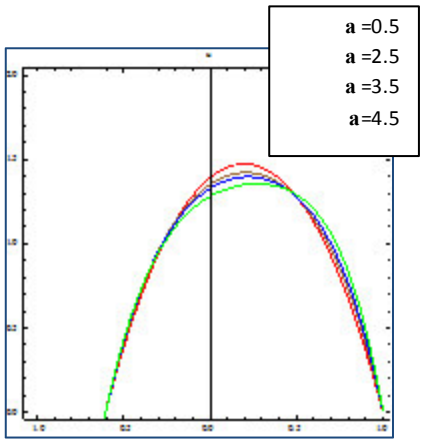

Fig.39.the velocity for different values of **a** at M=1.5,Re=5,Q1=1.1,Φ=0.5, a=0.2, b=0.2,d=0.5

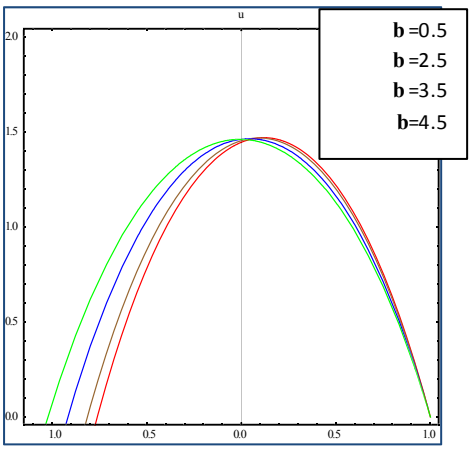

Fig.40.the velocity for different values of **b** at M=1.5,Re=5,Q1=1.1,Φ=0.5, a=0.2, b=0.2,d=0.5

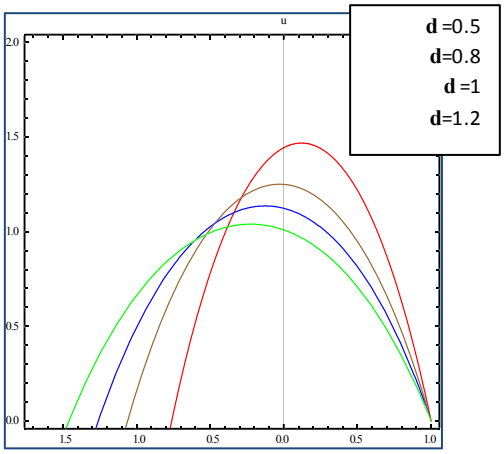

Fig.41.the velocity for different values of **d** at M=1.5,Re=5,Q1=1.1,Φ=0.5, a=0.2, b=0.2,d=0.5

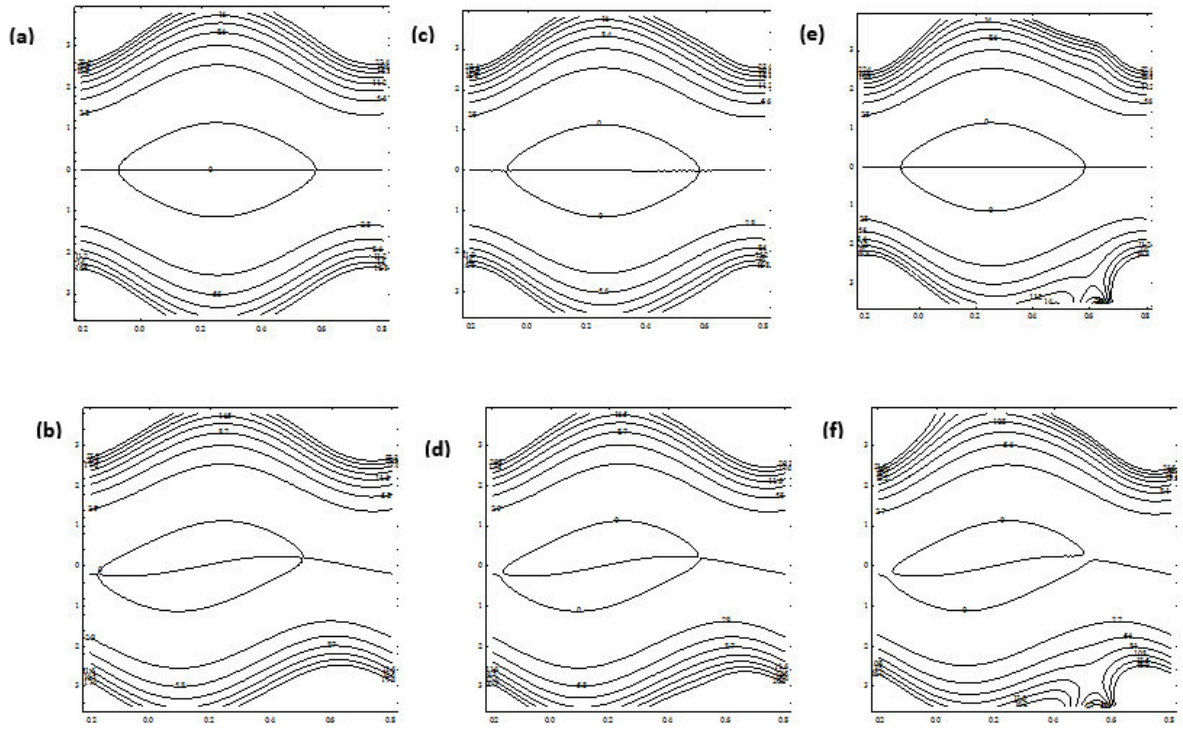

Fig.42. Streamline for different values of K: (a and b) K=0.5 ,(c and d) K=1.5, and(e and f) K=5.5, and Φ=0 at(upper panels) ,$\Phi=\frac{\pi}{3}$ at (lower panels) at Q1=1.5,d=1,a=0.5,b=0.5,M=1.2,Re=5, k1=5.5and $\beta=\frac{\pi}{6}$.

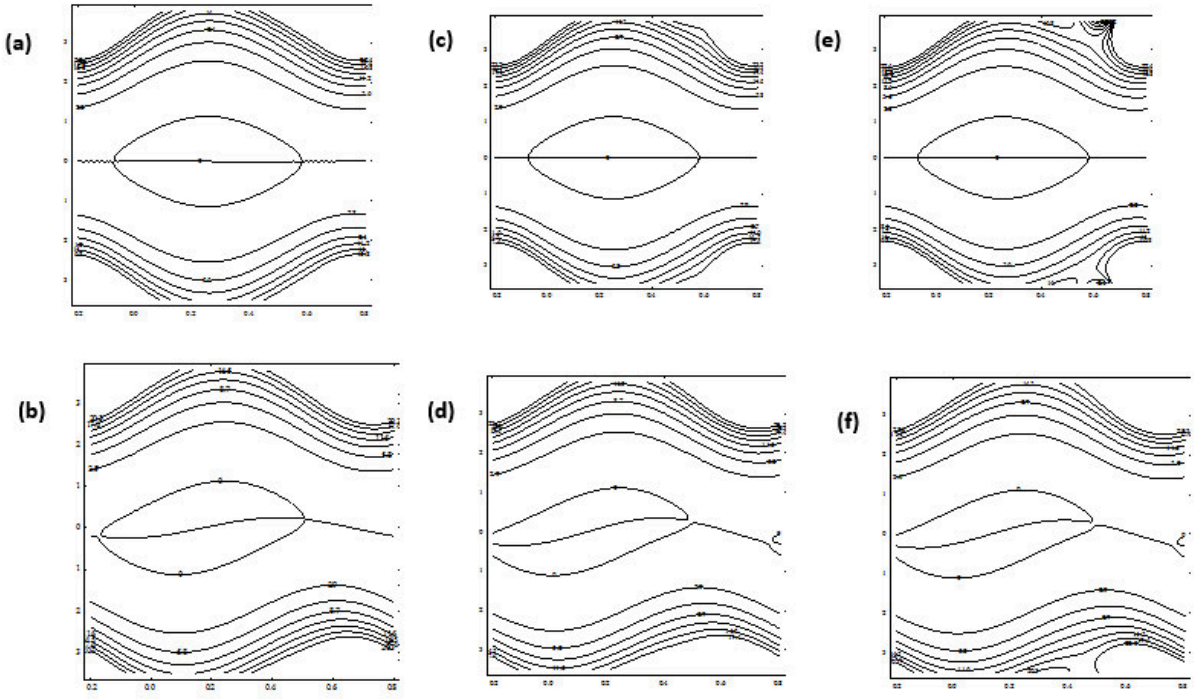

Fig.43. Streamline for different values of Re: (a and b) Re=5 ,(c and d) Re=10, and (e and f) Re = 15, and Φ=0 at(upper panels) ,$\Phi=\frac{\pi}{3}$ at (lower panels) at Q1=1.5,d=1,a=0.5,b=0.5,M=1.2,K=1, k1=5.5and $\beta=\frac{\pi}{6}$.

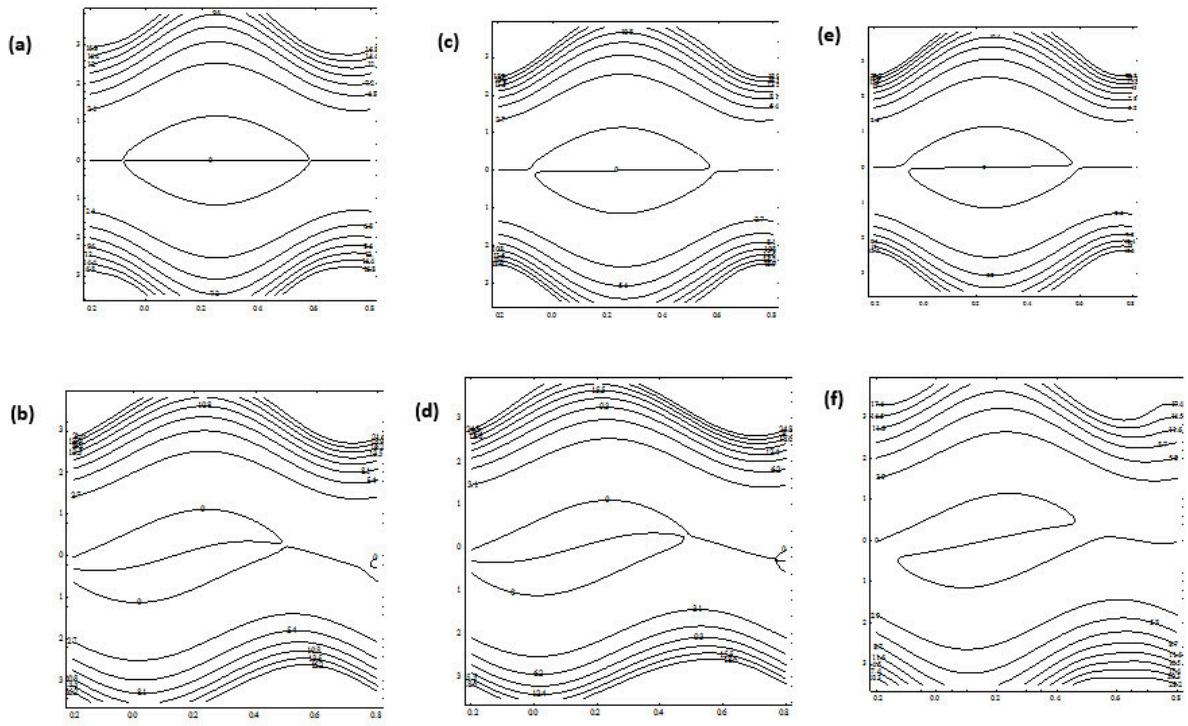

Fig.44. Streamline for different values of M: (a and b) M=0.5 ,(c and d) M=1, and (e and f) M = 1.5, and Φ=0 at(upper panels) ,$\Phi = \frac{\pi}{3}$ at (lower panels) at Q1=1.5,d=1,a=0.5,b=0.5,Re=5,K=1, k1=5.5and $\beta=\frac{\pi}{6}$.

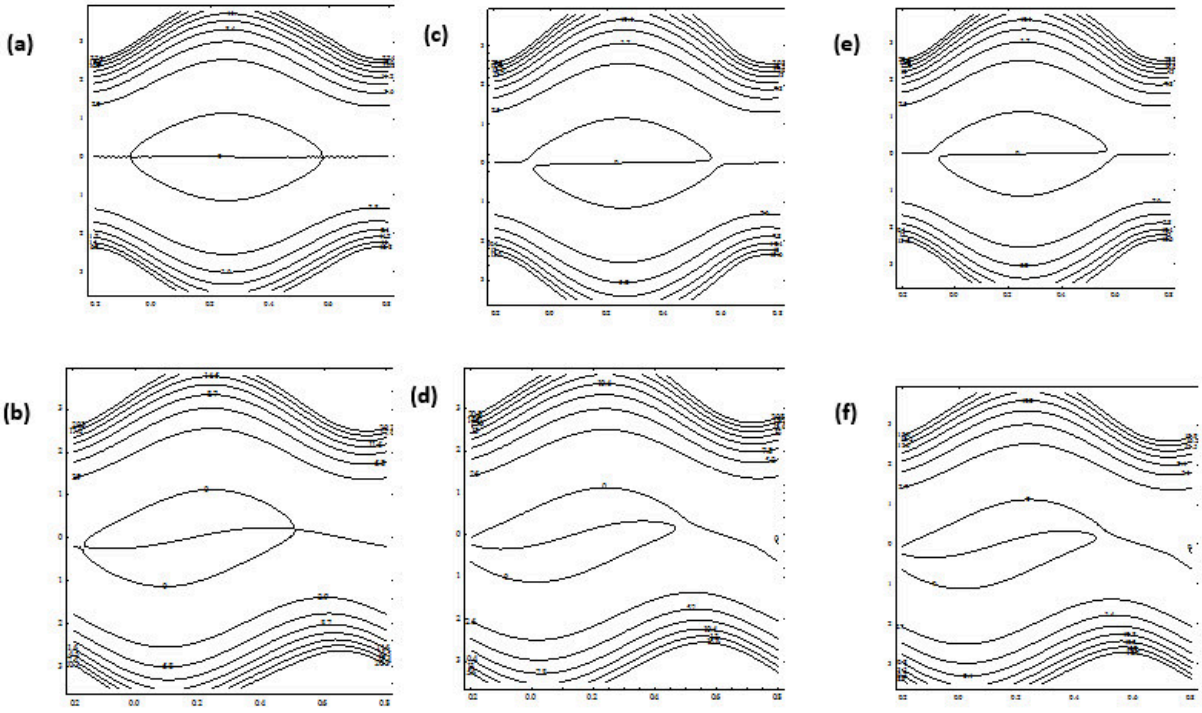

Fig.45. Streamline for different values of k1: (a and b) k1=0.5 ,(c and d) k1=1, and (e and f) k1 = 1.5, and Φ=0 at(upper panels) ,$\Phi=\frac{\pi}{3}$ at (lower panels) at Q1=1.5,d=1,a=0.5,b=0.5,Re=5,K=1, M=1.5and $\beta=\frac{\pi}{6}$.